

RESEARCH ARTICLE

Utilizing Machine Learning Algorithms to Predict Accuracy of the Index of Relative Tectonic Activity (IRTA), Dhansiri (North) River Basin in India and Bhutan

**SHAYANI ROY¹, PRITAM MANDAL², AMITAVA CHOWDHURY³,
M. ABDULLAH-AL-WADUD⁴, ARIYAN H. SEIKH⁵, AYAN H. SEIKH⁵,
MANOJIT GHOSH², AND ANANYA MUKHOPADHYAY¹**

¹Department of Earth Sciences, Indian Institute of Engineering Science and Technology (IIST), Shibpur, Howrah 711103, India

²Department of Metallurgy and Materials Engineering, Indian Institute of Engineering Science and Technology (IIST), Shibpur, Howrah 711103, India

³Department of Computer Science and Engineering, Pandit Deendayal Energy University, Gandhinagar 382007, India

⁴Department of Software Engineering, College of Computer and Information Sciences, King Saud University, Riyadh 11543, Saudi Arabia

⁵Department of Computer Science and Engineering, Motilal Nehru National Institute of Technology Allahabad at Prayagraj, Prayagraj 211004, India

Corresponding authors: Manojit Ghosh (mghosh.metal@faculty.iests.ac.in) and Ananya Mukhopadhyay (ananyageol@gmail.com)

This work was supported in part by King Saudi University, Riyadh, Saudi Arabia, through the Researchers Supporting Project under Grant RSPD2024R951.

ABSTRACT A river tries to maintain a dynamic equilibrium state by adjusting different controlling factors. A significant change in one of the controlling factors will dictate modifications in the others to re-establish the equilibrium in a river system. A river basin may indicate active tectonic movements more precisely than the best space-based geodetic techniques. Morphometric analyses, with the help of DEM and GIS often generates insights into the tectonic activities of an area. The Dhansiri (North) River basin lies on the north bank of the Brahmaputra and on the northern part of the Dhansiri-Kopili fault, which is tectonically active at different times. This paper analyses the impact of relative tectonics on drainage pattern development in the basin based on various morphometric parameters of linear (stream length ratio, bifurcation ratio), areal (form factor, basin elongation ratio), and relief (relief ratio, ruggedness number) aspects. Eleven well-known ML algorithms, namely, Logistic Regression (LR), K Nearest Neighbors (KNN), Random Forest (RF), Support Vector Machine (SVM), Decision Tree (DT), Gaussian Naive Bayes (GNB) classifier, Neural Network (NN), Extra Tree Classifier (ET), Ada Boost Classifier (AB), Gradient Boosting Classifier (GB), XG Boost Classifier (XGB) is used to model the spatial distribution of relative tectonic activity. These algorithms were executed in Python to assess prediction accuracy using standard metrics like accuracy, precision, recall, and F1 score. The assessment utilized widely used libraries such as sci-kit-learn and TensorFlow to implement and test the algorithms, benefiting from their comprehensive model evaluation and performance assessment tools. The SVM, ET, DT, and GNB techniques had the best performance, achieving an accuracy of 82.60 percent as per the modeling results. The Dhansiri (North) is a sixth-seven-ordered basin characterized by a dendritic drainage pattern. Notably, the spatial prediction of morphometric parameters with ML is potentially competent for regional analyses of neotectonics.

INDEX TERMS Morphometric parameters, index of relative tectonic activity, tectonics, Dhansiri (North) river basin, machine learning algorithms.

I. INTRODUCTION

The associate editor coordinating the review of this manuscript and approving it for publication was Mauro Gaggero¹.

A River that strives to maintain a dynamic equilibrium state is known as a graded river, which exhibits a characteristic

feature where any change to one of its regulating variables leads to a corresponding alteration in another variable to restore equilibrium. The evolution of landforms and drainage networks is believed to be controlled by a specific region's tectonic evolution and structural deformation, supported by numerous theoretical models and field observations. In low-relief areas, the assessment of tectonic activity can be achieved through a comprehensive analysis of the dynamics of alluvial rivers, as suggested by [1]. Geomorphometry, in its simplest form, is the extraction of (land) surface attributes (morphometric, hydrological, climatic, etc.) and objects (watersheds, stream networks, landforms, etc.) [2], [3]. Since the publication of historical studies on drainage basin morphometry by [4], [5], and [6] the morphometry-based method has gained popularity in geomorphology. Following this well-accepted approach, a large number of studies were conducted in the last decade [7], [8], [9]. They have demonstrated that morphometry-based indicators may be used to identify the presence of active tectonics [10], [11], [12], [13], [14], [15]. Morphometric analysis has become a popular method in geological research worldwide, with numerous studies conducted in countries such as the USA [16], Spain [17], Italy [18] Pakistan and Afghanistan [19], Iran [20], [21], Slovakia [22], Poland [23], Turkey [24], Greece [25] but also in India [26], [27], [28]. Morphometry refers to the measurement and mathematical analysis of the shape, configuration, and dimension of landforms on the surface of the earth [29]. The morphometric characteristics of a drainage basin can provide valuable insights into the underlying geology, climate, relief, and tectonics of a watershed. In the field of geomorphology, there has been a significant focus on developing quantitative physiographic methods to study the evolution and behavior of surface drainage networks [5]. Rivers aim to maintain a dynamic equilibrium, wherein any changes to one of their controlling factors result in corresponding adjustments to restore balance. The fluvial landscape is influenced by various factors such as lithology, climate, and tectonics, and alterations in any of these can significantly impact the system. Mountainous regions are particularly vulnerable to natural disasters like landslides, earthquakes, and flash floods, which can result in substantial economic and property damage. To mitigate these risks, various predictive models have been developed for landslide susceptibility mapping using statistical [30], [31], [32], [33], and probabilistic techniques [34], [35], [36].

As river geometry and fluvial sediments are sensitive indicators of neotectonic activity, their response to tectonic forces can be relatively rapid and readily visible in the landscape. Deciphering a river basin's morphometric characteristics is the most reliable proxy for tectonics and their impact on basin areas [37]. Both quantitative and qualitative approaches are used to study these proxies, and GIS technology is an effective tool for examining different drainage morphometric features [38]. Despite the availability of advanced space-based geodetic techniques,

detecting changes in river basins can be more precise for identifying neotectonics. On the other hand, there might be more significant difficulties in detecting active tectonic movements. Different empirical techniques for predicting spatial changes in river basins can be challenging to implement due to their high computational time, complexity, and efficacy requirements, leading to increased costs. Spatial data such as geology, geomorphology, and morphometric data are potentially beneficial to explain the generated maps based on the value of the variable and spatial dependence. In contrast, machine learning (ML) algorithms have gained prominence in spatial prediction studies [39]. Among the advantages of ML are the possibility of testing various statistical algorithms, working with non-linear data without spatial dependence, and include auxiliary factors in the prediction [30], [40]. In the natural environment, non-linearity and higher-order interactions make traditional statistical models unsuitable. However, Artificial Intelligence (AI), specifically Machine Learning (ML), has the potential to address these issues by identifying strong links in data and learning complex nonlinear mappings from high-dimensional eigenvectors to the desired output using a standard training dataset. Numerous studies have established the capability of ML to discriminate geomorphic and land cover classes; using multi or hyper-spectral reflectance data ([41], [42], [43], [44], [45]). Several of the classification studies established the potential of Support Vector Machine (SVM) for the discrimination of lithological units ([46], [45], [47], [48], [49]).

Despite being widely accepted in other fields, there has been limited adoption of ML applications in the Earth science community. This study aims to systematically analyze the drainage morphometry and reconstruct the evidence of neotectonic control on the Dhansiri(North) River Basin using geographical information systems, remote sensing techniques, and Logistic Regression (LR), K nearest neighbors (KNN), Random Forest (RF), Support Vector Machine (SVM), Decision Tree (DT), Gaussian Naive Bayes classifier (GNB), Neural Network (NN), Extra Tree Classifier (ET), Ada Boost Classifier (AB), Gradient Boosting Classifier (GB), XG Boost Classifier (XGB) ML models. Logistic Regression (LR) is a statistical method used for binary classification tasks, predicting the probability of an instance belonging to a particular class using a logistic function. LR is particularly suitable for scenarios where the outcome is binary, such as predicting whether the value of IRTA is low or high. On the other hand, KNN operates by classifying data points based on the majority class of its nearest neighbors. It doesn't construct explicit models but rather stores training data instances and classifies new cases based on their similarity to existing data points. K Nearest Neighbors (KNN) is effective for both simple and complex classification tasks because it's non-parametric and does not assumptions about the underlying data distribution. Random Forest(RF) is an ensemble learning method that builds multiple decision trees

during training and outputs the class, which is the mode of the classes of the individual trees. This ensemble approach helps reduce overfitting and improves the model's performance, while Support Vector Machine (SVM) is a powerful supervised learning algorithm used for classification tasks. SVM finds the hyperplane that best separates classes in the feature space, making it suitable for both linear and non-linear problems through kernel functions. Decision Tree (DT) creates a tree-like structure by recursively splitting data based on features. Each internal node represents a "test" on an attribute, each branch represents the outcome of the test, and each leaf node represents a class label. Gaussian Naive Bayes (GNB) Classifier is a probabilistic classifier that assumes feature independence, making it particularly effective for text classification tasks where each feature (word) is treated independently. Neural Networks (NN) are computational models inspired by the human brain's structure and function. They consist of interconnected layers of nodes (neurons) that transmit signals between each other. Neural networks can learn hierarchical representations of data, making them suitable for complex tasks like image recognition and natural language processing. An Extra Tree Classifier (ET) is an extension of the RF algorithm that introduces randomness at the splitting point, further reducing variance and potentially increasing bias. Ada Boost (AB) and Gradient Boosting (GB) are boosting algorithms that sequentially combine weak learners to create a strong learner. Ada Boost assigns weights to misclassified instances, while Gradient Boosting builds trees sequentially, correcting errors made by previous models. The XG Boost Classifier (XGB) is an optimized implementation of Gradient Boosting known for its efficiency and accuracy. It features parallel processing and regularization techniques to improve performance and prevent overfitting. While previous studies have explored morphometric parameters about neotectonics, there has yet to be an exploration of using ML to predict these parameters. The study focuses on the Dhansiri (North) river basin, located on the north bank of the Brahmaputra valley in the lower section of Assam. This area is considered one of the world's most complex geological and tectonic regions. The basin's drainage characteristics are susceptible to any changes in the geological activity of the region, making it an ideal location for examining the effects of geomorphological and geological processes on the development of drainage patterns. To achieve this, the study uses various morphometric parameters, including linear and areal parameters and relief parameters.

The primary objective is identifying evidence of neotectonic control in the river basin using various morphometric parameters and predictive approaches based on machine learning algorithms. We used eleven different ML algorithms to compare and assess the efficiency of these algorithms to establish the criteria choice in terms of input parameters and classifiers for IRTA mapping. It should be noted that while many studies have focused on neotectonics and morphometric parameters, more research is needed on predicting

these parameters using machine learning algorithms. So, the main goal of this study is to fill the observational gap in neotectonic studies in an area, which is not covered by most of the neotectonic investigations in northeast India.

II. STUDY AREA

A. GEOLOGY, STRUCTURE, AND TECTONICS

The geological and tectonic zones in the northeastern region of India, including the Himalayan fold belt, the Naga-patkai Ranges, the Shillong plateau, and the Brahmaputra Valley in Assam, are very complex and diverse. The study region, Dhansiri (North) river basin area is located above the active Kopili fault in Brahmaputra valley region. This basin area consists of various metamorphic and sedimentary sequences belonging to different period, ranging from Neogene to Quaternary (Figure 1). The predominant rock types in this region are gneiss, conglomerate, pebbly sandstone and oxidized dark brown to red-brown loamy sand, unconsolidated, unoxidized sand, silt, and clay (Table 1). Due to the different characteristics of the lithologies, their effect on the drainage patterns, including the deformations, can also differ. The Dhansiri-kopili fault and the Atherkhet fault are two major tectonic features in the study area (Figure 2), and they are primarily neotectonic faults. When a river enters an alluvial plain in a tectonically active region, it may accumulate a thick sequence of poorly sorted sediments, including gravel, sand and silt. According to geological age, the basin area sequentially consists of lithological properties from the early Pleistocene to the Meghalayan period after crossing the main boundary thrust. However, in the river's middle reaches, the figure 1 shows unconsolidated sand, silt, clay in the deposition of quaternary sediments, possibly during the Meghalayan (Last 4200 years BP) period. These quaternary sediments provide Stratigraphic evidence for delineating the significant phases of neotectonic activity near the Main Frontal Thrust, The Atherkhet fault, and The Dhansiri-Kopili fault. The basin area is a primarily aseismic region, characterized by earthquakes from 1963 to 2022 with different magnitudes. The lithology and structure of these geological formations significantly impact the geomorphology of the basin.

TABLE 1. Lithological characteristics.

Formations	Age	Group	Lithological Characteristics
Barpeta-I	Meghalayan	Newer alluvium	white to greyish sand, silt, pebble and clay.
Barpeta-II	Meghalayan	Newer alluvium	Un-stabilized, unoxidized sand, silt and clay
Chapar	Middle-late pleistocene	Older alluvium	highly oxidized dark brown to red brown loamy sand
Corramore	Early Pleistocene	Older alluvium	gneiss/quartzite pebbles in oxidized sand, silt, clay
Hauli	holocene	Newer alluvium	Un-stabilized, unoxidized sand, silt and clay
Kimin	Pliocene-pleistocene	Sivalik	Pebbly sandstone, conglomerate bands with clay
Sorbhog	Pleistocene-holocene	Older alluvium	oxidised to feebly oxidised sand, silt and clay
Subansiri	Miocene-pliocene	Sivalik	SST, calcareous nodules, carbonised wood, coal seam

B. REGIONAL SETTINGS

The One of the tributary basins of the Lower Assam area of India's Brahmaputra river is the Dhansiri (North) river basin. This region (Figure 3) is bordered to the north by Bhutan and the West Kameng district of the Arunachal Pradesh state, to the east by Sonitpur district, to the south by Darrang district, and to the west by Baksa district. The 2404 km² Dhansiri (North) basin (26°29'11" to 27°18'30" N, 91°47'15"

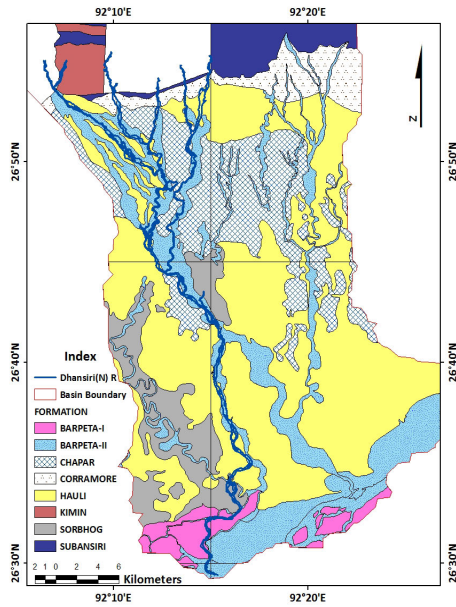


FIGURE 1. Lithological characteristics.

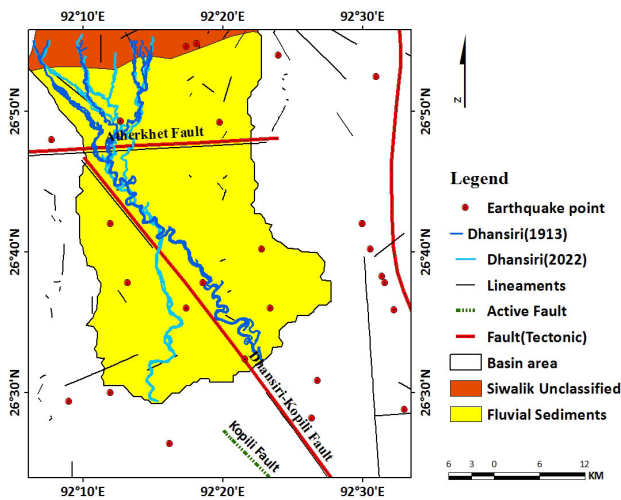


FIGURE 2. Seismotectonic map.

to 92°27'45" E) resides on the northern portion of the Kopili fault and the north bank of the Brahmaputra, both of which are tectonically active at different times.

The Dhanisiri(North) river is almost 103 km long originated from Trashigang and Samdrupjongkhar district border region, Bhutan and meets river Brahmaputra near dalgaon town of Darrang district, Assam.

III. MATERIALS AND METHODS

This section thoroughly explains the study's data collecting, analysis, and research design methods.

A. DATA: COLLECTION AND PROCESSING

The current study is based on Survey of India (SOI) topographic maps (<https://surveyofindia.gov.in/>) with the

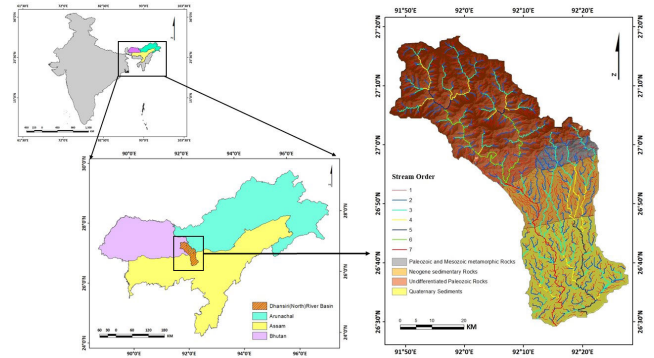


FIGURE 3. Location of the study area.

TABLE 2. Materials used.

Materials used		Year	Scale	Source	
Toposheets (78M/15, 78M/16, 78N/13, 83A/3, 83A/4, 83A/8, 83B/1, 83B/2, 83B/5, 83B/6)		1912-13 2005-09	1:63,360 1:50,000	Survey of India, 1931 and 2009	
Satellite	Sensor	Path / Row	Resolution	Date of acquisition	Source
Landsat 8	OLI-TIRS	136/41, -42	30 m	18.01.2023	Earth Explorer-USGS
DEM	SRTM	136/41, -42	90 m	11.01.2000	Earth Explorer-USGS
Materials used		Scale	Source		
Geological, lithological, lineaments, faults & seismic data		1:50,000	Bhukoshi-GSI		

numbers 78M/15, 78M/16, 78N/13, 83A/3, 83A/4, 83A/8, 83B/1, 83B/2, 83B/5, and 83B/6 on the scales 1:63360 and 1:50,000 from 1913 and 2009, respectively. A spatial scale of 1:63,360 means 1 inch on the map represents 1 mile on the ground. On the other hand, 1 centimeter on the map represents 50,000 centimeters (or 500 meters) on the ground, then it is considered as 1:50,000 scale map. With the aid of the Geomatica 2012 software and the Global/World Geodetic System (WGS), which dates back to 1984 and was last amended in 2004, topographical maps were referenced geographically, mosaiced, and the whole research region was outlined in a GIS environment. Geological, lithological, lineaments, faults, and seismic data were obtained from Bhukosh-GSI (<https://bhukosh.gsi.gov.in/Bhukosh/MapView.aspx>) to better comprehend the tectonic effect on the research region. Lithological map has been prepared by field traverse which supports the Bhukosh-GSI data and different geological investigations. The digital data base for the drainage layer of the basin was created using a variety of characteristics that were derived from an SRTM DEM with a spatial resolution of 90m (<https://earthexplorer.usgs.gov/>) (Table 2).

The morphometric study of a drainage basin is next presented. The drainage basin was digitised for morphometric analysis in a GIS utilising Arc GIS 10.3.1 and TNT Mips 2021 software, and it calls for the delineation of all the already existing streams. By employing a stream ordering approach [6], the basin is made up of subbasins with stream orders ranging from first to seventh. The study area is divided into 115 sub basins of 3rd or 4th order streams. Highest number of first-order streams is observed near the basins, which are falling close to segment of faults. Eleven distinct ML algorithms' prediction accuracy was calculated

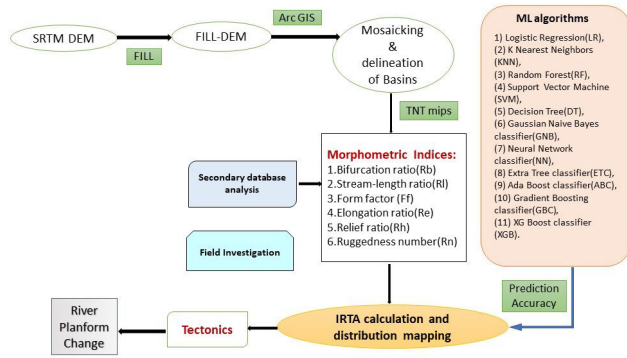


FIGURE 4. Work flow in neotectonic studies along with ML.

TABLE 3. Mathematical derivation and description of morphometric parameters along with the classification using previous literatures.

Types of Parameters	Parameter Nomenclature	Mathematical Derivation	Description	Classes Ranges Adopted	References
Linear	Bifurcation Ratio (R _b)	N_u/N_{u+1}	N _u = Total number of stream segment of a particular order N _{u+1} = number of segments of next higher order	Class 1 <: 1.821 Class 2 >: 1.821	Horton, 1932
Linear	Stream Length Ratio (R _L)	l_u/l_{u-1}	l _u = Total stream length of particular order u l _{u-1} = Total stream length of next lower order	Class 1 <: 2.859 Class 2 >: 2.859	Horton, 1945
Areal	Form Factor (F _f)	A/L_b^2	A = Basin Area L _b = length of basin	Class 1 <: 0.0281 Class 2 >: 0.0281	Horton, 1932
Areal	Elongation Ratio (R _e)	$R_e = 2(A/\pi)^{0.5}/L_b$	A = basin area L _b = Maximum Length of the basin	Class 1 <: 0.23 Class 2 >: 0.23	Schumm, 1956
Relief	Relief Ratio (R _h)	H/L_b	H = Basin Relief L _b = Length of the basin	Class 1 <: 0.03 Class 2 >: 0.03	Schumm, 1956
Relief	Ruggedness number (R _n)	$R = D_d$	R = Basin Relief D _d = Drainage Density of the basin	Class 1 <: 2.807 Class 2 >: 2.807	Strahler, 1957

using Python programming (python 3.8) in Jupiter Notebook (notebook version 6.5.2). Later field evidences were collected to identify the evidences of tectonic activities. A flowchart (Figure 4) on data processing applied for the work is shown below-

B. MORPHOMETRIC ANALYSIS

The present study evaluates the landforms of the basin area, through morphometric analysis to identify the presence of any evidences of neotectonics. The total river system in the area is extracted from SRTM-DEM. The DEM data was used to measure the (1) Linear, (2) Areal, and (3) Relief aspects for the analysis are necessary for the systematic study of drainage basin features as well as tectonically derived features. The description of morphometric parameters are explained (Table 3).

The research design is to analyze different parameters in sub basins of the Dhansiri(North) River basin, then break them into tectonic classes based on the values of individual parameters. We divide the various indices into two classes based on a threshold value, with one being high tectonic activity and another class being low activity (Table 4). Here, the threshold values are the average values of each parameter. Then, the class of these parameters is summed, averaged, and divided into Index of Relative Tectonic Activity classes over the study area(Table 5).

C. EXPERIMENTAL SETUP

In this survey, six independent morphometric parameters from different aspects such as Bifurcation Ratio (R_b), Stream

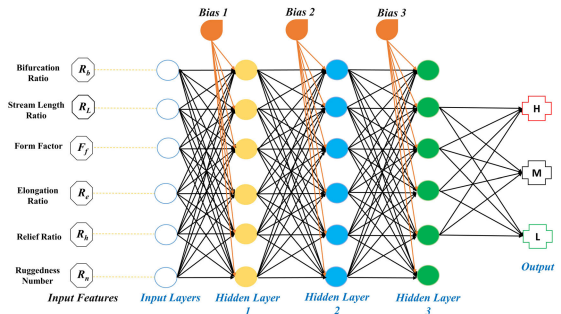


FIGURE 5. An architecture of a multi-layer feed-forward neural network consisting of an input layer, three hidden layers, and one output layer, along with the Six input features and three bias nodes.

Length Ratio (R_L), Form Factor (F_f), Elongation Ratio (R_e), Relief Ratio (R_h), and Ruggedness Number (R_n) were used to predict the Index of Relative Tectonic Activity (IRTA) using eleven well-known ML algorithms, namely, (1) Logistic Regression (LR), (2) K Nearest Neighbors (KNN), (3) Random Forest (RF), (4) Support Vector Machine (SVM), (5) Decision Tree (DT), (6) Gaussian Naive Bayes classifier (GNB), (7) Neural Network classifier (NN), (8) Extra Tree classifier (ETC), (9) Ada Boost classifier (ABC), (10) Gradient Boosting classifier (GBC), (11) XG Boost classifier (XGB). In the study evaluating eleven machine learning algorithms in Python, the criteria used to assess prediction accuracy included standard metrics such as accuracy, precision, recall, and F1 score. The evaluation process leveraged popular libraries such as sci-kit-learn and TensorFlow for implementing and testing the ML algorithms. These libraries provided robust tools for model evaluation and performance measurement. Based on the IRTA class, a dataset comprising 115 different data was divided into three categories; low, medium, and high, according to their ranks (Figure 5).By dividing the parameters into these classes, researchers can discern patterns and correlations between the geological characteristics of the sub-basins and the tectonic activity levels. The ranks were assigned based on the highest relative closeness value to the lowest value with the help of linear, areal and relief morphometric parameters. This approach helps understand how tectonic activity influences the hydrological and geomorphological features of the river basin, which is crucial for various applications such as land use planning, hazard assessment, and environmental management. The entire dataset was then divided into two categories: training and testing. 80 percent of the total dataset, that is, 92 data, were chosen arbitrarily for training, and the remaining 20 percent, or 23 data, were retained for testing.

IV. RESULTS AND DISCUSSION

A. MORPHOMETRIC PARAMETERS

In tectonic geomorphology, morphometric parameters refer to measurements and characteristics used to quantify the shape, form, and relief of landscapes and landforms that have been influenced by tectonic processes. Morphometric

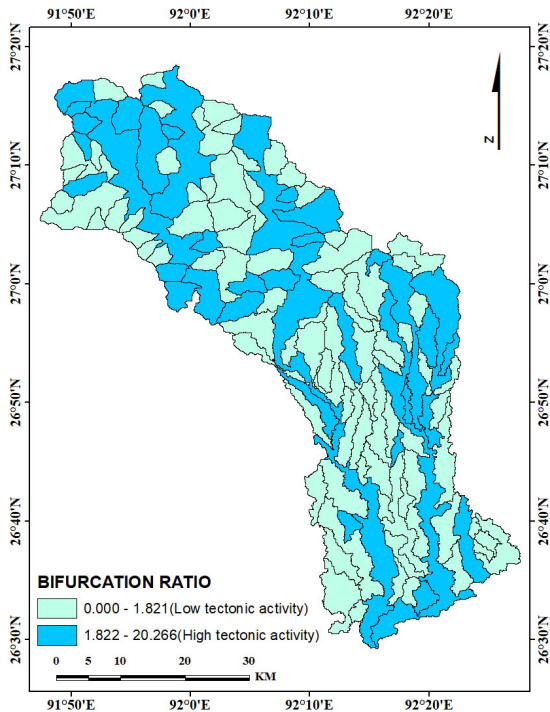


FIGURE 6. Bifurcation ratio.

parameters detect anomalies in the fluvial system. These anomalies may be produced by local changes from tectonic activity resulting from uplift or subsidence. The main goal of this study is to evaluate and quantify the role of neotectonics in the lesser Himalayan zone. The investigation of the present study is to decipher the role of neotectonics in the 2404 km^2 area on 115 basins using Linear, Areal and Relief parameters with ML algorithms.

1) LINEAR PARAMETERS

The linear parameters have been evaluated using Stream characteristics, including the number and length of streams of various orders, total stream length, mean stream length, and level of dissection, have an impact on the hydrological characteristics of a basin. This analysis aims to define the basin's evolution as one-dimensional characteristics using the bifurcation ratio and stream length ratio as parameters for evolution. The main channel-Dhansiri(North) River, belongs to seventh order stream. According to [4], basic variables such as stream length and stream count are geometrically linked to stream order.

α : BIFURCATION RATIO (R_b)

(R_b) is the proportion between the total numbers of drainages of one sort to that of the next upper order in a drainage basin and so on. The (R_b) varies depending on the characteristics of the drainage basin. The bifurcation Ratio varies between 3 and 5 for natural drainage system in which geologic formations modify the drainage pattern. (R_b) typically has a minimum value of 2 for flat or rolling drainage basins

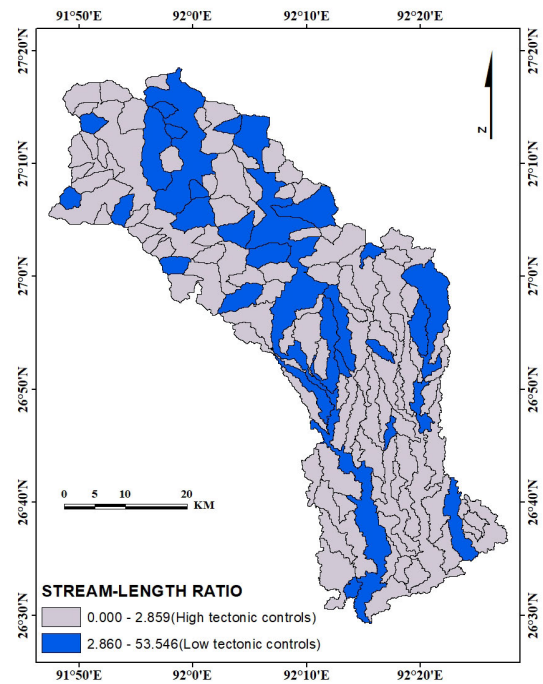


FIGURE 7. Stream length ratio.

[5], suggesting a more straightforward and less branching structure. In contrast, (R_b) in mountainous or highly dissected drainage basins can vary from 3 to 4, suggesting a more complicated and branching drainage pattern caused by the rough terrain and variable topography.

$$R_b = \frac{N_U}{N_U + 1}$$

where, N_U is total number of stream segments of a particular order and $N_U + 1$ are the number of segments of the next higher order. The mean values of all these ratios lead to the bifurcation ratio. The average bifurcation ratio of the river basin is- 3.615. High mean bifurcation ratio indicate area influenced by structural disturbances, represented by fault system, tectonic activity, and rejuvenation phases. The higher values of (R_b) represent youth stage while lower values represent a mature stage of basin development. The 115 subbasins in the research region had (R_b) values ranging from 1 to 20.26. According to the values for this parameter, the basin area was divided into two classes: class-1 included sub-basins with $R_b \leq 1.821$ and class-2 included sub-basins with $R_b \geq 1.821$. (1.821 is the mean value of the total of the 115 sub-basins). The geographical distribution of this variable is depicted in (Figure 6). Overall R_b values indicate that 26% of the basin area influenced by structural disturbances, represented by fault system, high tectonic activities. 74% of the area related to the class 1(except basin no:6,11,21,22,29,31,32,38,39,41,44,55,56, 58,61,70,78,79,90,93,96,97,99,100,110,112,113,115),with low tectonic activities. Here, the mentioned basins are under the area of high tectonic controls.

b: STREAM LENGTH RATIO (R_L)

Following [5]’s method, the average stream length segments of each of the successive orders of a basin follow a direct geometric series with L_U , which increases towards a higher order of streams. The (R_L) value between streams of different order reveals that there are variations in slope and topography.

$$R_L = \frac{L_U}{L_U - 1}$$

where, L_u is the total stream length of the order ‘u’ and L_{u-1} is total stream length of its next lower order. Here (Figure 7), values vary from 0.406 to 53.546 and the mean value is 2.859. The value categorized into two classes to determine the tectonically active basin. Class 1 having basins with $R_L \leq 2.859$, suggest that basins are tectonically controlled. On the other hand, class 2 is related to the basins having $R_L \geq 2.859$. Basin no 1,6,11,16,21,29,32,41,44,45,50,56,59,68,70,79,83, 85,86,89,90,91,99,103,105,109,112 associate with class 2 with low tectonic controls, rest of the basins are associated with high tectonic controls(class 1).

Mean Stream Length Ratio (R_{LM}): The (R_{LM}) of the Dhansiri river basin is 5.674. The overall value of ‘(R_L)’ shows the area is below the (R_{LM}) value, a decreasing trend in ‘(R_L)’ from higher order to lower order. This indicates the youth stage of geomorphic development of river and affected by the tectonic activity.

2) AREAL PARAMETERS

The areal parameters include Form factor, Elongation ratio are evaluated to interpret the erosional activity of the basin. The shape of the drainage basin is characterized by elongation ratio and form factor. The lower value of the elongation ratio and form factor indicate elongated basins, which suggest the basins are tectonically active.

a: FORM FACTOR (F_f)

It is defined as the ratio of basin area to the square of the basin length [4]. The watershed with high form factor values have the high peak flows for shorter duration, whereas elongated watershed with low form factor values will have a flatter peak of flow for later duration. Thus, it can be expressed as

$$F_f = \frac{A}{L_b^2}$$

where (F_f): Form factor, A: Watershed Area, and L_b : length of the watershed. The mean form factor of the 115 sub-basins of Dhansiri river basin is 0.0557sq. km, which indicates that the basin is more elongated in shape, which claimed to develop in tectonically more active areas. Here (Figure 8), values range from 0.006 to 0.432. Mean value is 0.0281. The mean value is the threshold value for classifying the data into two classes-high and low tectonically active areas. Basin no 1,2,5,6,12,19,20 31,32,33,34, 35,37,38,39,40,75,76,77,78,79 belongs to class 2 ($F_f \leq 0.028$), which indicate the elongated basins are moderate tectonically active. 81% area of the basin

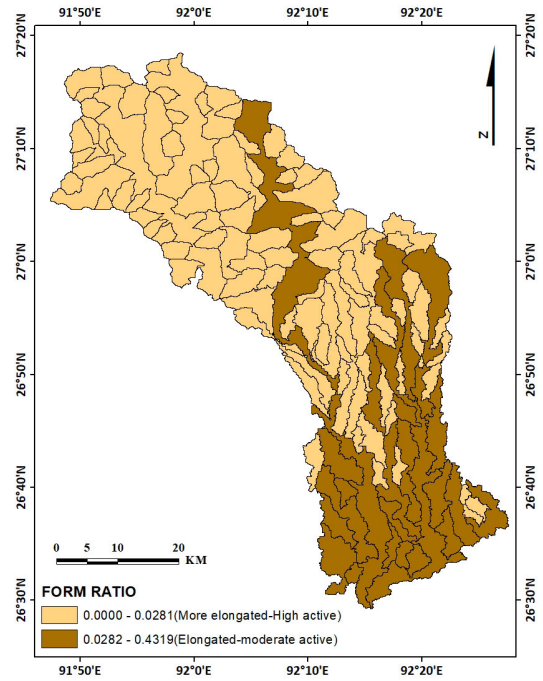


FIGURE 8. Form ratio.

is associated with Class 1, which indicate the more elongated basins are under high tectonically active zone.

b: ELONGATION RATIO (R_e)

R_e represents the watershed shape of any river. [50] defined R_e as the ratio of the diameter of a circle having the same area as the watershed and the maximum watershed length (L_b). It may be obtained by using the formula

$$R_e = 2 \left(\frac{A}{\pi} \right)^{0.5} / L_b$$

where ‘ R_e ’ is the elongation ratio, ‘2’ is a constant, ‘A’ is the area, and ‘ L_b ’ is the maximum watershed length. The value of R_e varies from 0 (highly elongated shape) to unity i.e. 1.0 (circular shape). The mean ‘ R_e ’ value of 115 sub-basins is 0.26, which means the more elongated basin area indicate high tectonic activity. Values range from 0.03-0.74 and the values are grouped into two classes including class 1 having sub-basins have values $R_e \leq 0.23$ and class 2 consist of sub-basins have $R_e \geq 0.23$ (0.23 is Mean value). Basin no. 1, 2, 31, 32, 33, 34, 35, 37, 40, 75, 76, 77 link with class 2 with moderate tectonic activity. (Figure 9). 88% basins are associated with class 1, structurally and tectonically controlled.

3) RELIEF PARAMETERS

Relief ratio, Ruggedness number are interpreted parameters of the study area to evaluate the denudation characteristics of the basin. The relief ratio defined as the ratio of basin relief to the length of the basin. The lower value of relief ratio is characteristic feature of less resistant rocks and vice versa. The lower value of Ruggedness number implies the basin area

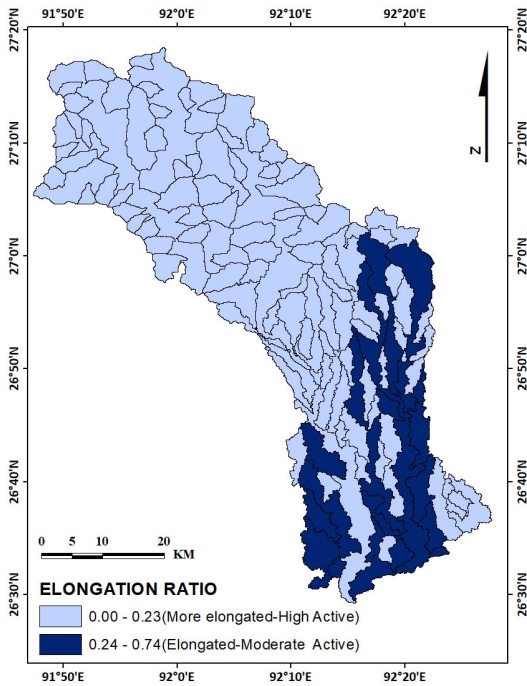


FIGURE 9. Elongation ratio.

is less prone to soil erosion and disposed to intrinsic structural complexity.

a: RUGGEDNESS NUMBER (R_n)

Ruggedness number (R_n) is the product of drainage density and maximum relief (difference between the highest and lowest) of the basin [50]. It is defined as:

$$R_n = R * D_d$$

R is the basin relief, D_d is Drainage density of the basin. Its higher values occur when the slope of the basin are not only steep but also long as well. The mean R_n value of the sub-basins of Dhansiri basin is 5.571276, which means high (R_n) values correspond to this basin with rough relief possibly affected by tectonic uplift, whereas low values usually indicate tectonic stability or slow rates of uplift. The range of R_n for this research region is 0.01 to 73.95, with the mean values of the basins being 2.807. According to the values of these parameters, the basins in the research region were divided into two classes: class 1 included basins with $R_n \leq 2.807$ and class 2 included basins with $R_n \geq 2.807$. Basins related to class 2 are (basin no 10, 11, 31, 32, 42, 44, 59, 60, 72, 114 and 115) are influenced by high tectonic activity. (Figure 10).

b: RELIEF RATIO (R_h)

The difference between the highest height and lowest height in any basin is known as Relief (H). According to [50], the R_h is the ratio of total basin relief to the longest dimension (L_b) of the basin, which tends to parallel the main drainage. The R_h computes the overall steepness of any watershed to analyze

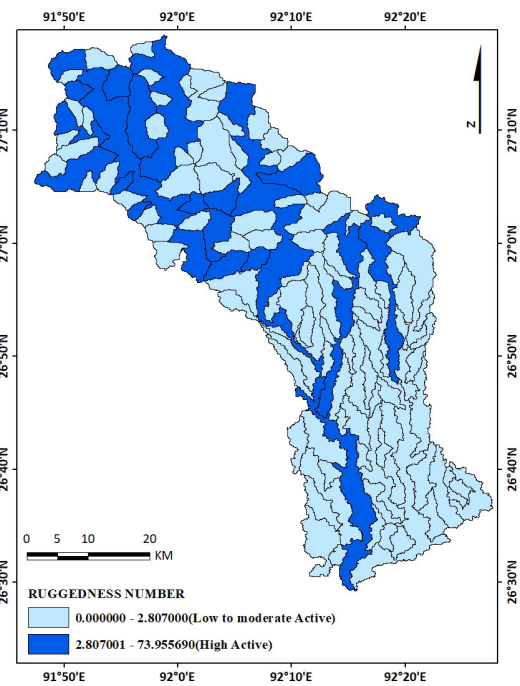


FIGURE 10. Ruggedness number.

the effectiveness of degradational processes that operate on basin slopes and are proportional to the surface run-off and intensity of erosion.

$$R_h = \frac{H}{L_b}$$

The average value of the 115 sub-basins is 0.05, which is considered as a higher value for this basin, which explains steeper slopes and high relief, as indicators of higher tectonic activity. The 115 sub-basins are divided into two classes based on their R_h values: class 1 includes basins with $R_h \leq 0.03$ and class 2 includes basins with $R_h \geq 0.03$ (0.03 is the mean value of the sub-basins). R_h values range from 0 to 0.38. The geographical distribution of the R_h values for the river basin region is shown in (Figure 11). High values from class-2 are displayed in basins 9, 10, 11, 31, 50, 56, 72, 79, 90, 99, 100, 101, 102, 104, 105, 107, 110, 114, and 115. Moreover, overall R_h values point to increased tectonic activity.

B. INDEX OF RELATIVE TECTONIC ACTIVITY (IRTA)

The six calculated morphometric parameters are combined and the average of their class number (1 or 2) revealed a new integrated index named the Index of relative tectonic activity (IrtA), which results from formula. This method is used to improve the accuracy of the evaluation of the relative tectonic activity in the study area:

$$IRTA = (R_L + R_b + F_f + R_e + R_n + R_h)/n$$

The drainage basin was divided into three groups of relative tectonic activity: low (1), moderate (2), and high (3) based on

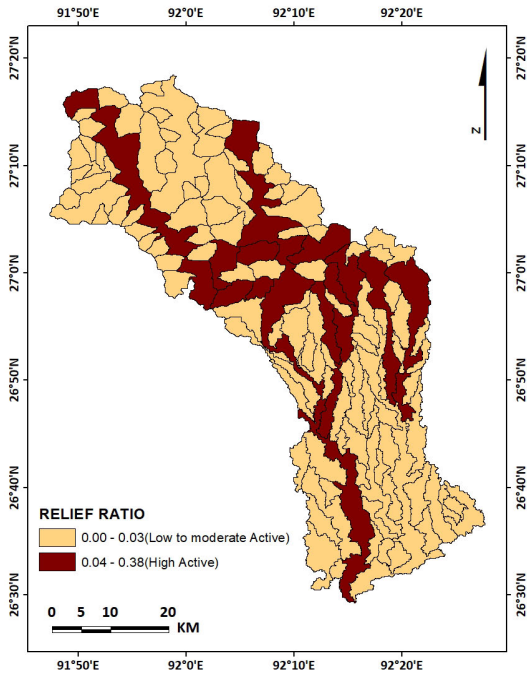


FIGURE 11. Relief ratio.

the revised index values. In order to make inferences about the tectonic structure of the research region, a map depicting the geographical distribution of the values of this index was created. Irta values were categorised into three groups based on the level of relative tectonic activity: basins with low tectonic activity are classified as Class 1 ($1 \leq IRTA \leq 1.25$), catchments with moderate tectonic activity are classified as Class 2 ($1.26 \leq IRTA \leq 1.50$), and basins with high tectonic activity are classified as Class 3 ($1.51 \leq IRTA \leq 2$). The outcomes of the drainage basins' categorization discussed above are shown in (Figure 12). Analysis of the study area's 2404 km^2 has revealed that roughly 68% of it is under Class 1, about 23% falls under Class 2, and about 9% falls under Class 3. The geological structure of the research region appears to be reflected in how this new index's values are distributed spatially. High relative tectonic activity has an impact on the river morphology of both the Dhansiri-kopili fault and the Atherkhet fault segment areas.

C. PREDICTION OF CLASSIFIED IRTA

The model's accuracy validations and the number of true and false predictions made by a classifier can be summarised by a confusion matrix, as shown in Figure 13. It can be clearly seen from Image, that the accurately predicted regions of the matrix are matrix cell (0×0) for High IRTA, (1×1) for Medium IRTA and (2×2) for Low IRTA. So, High IRTA = 0 (0×0) , Medium IRTA = 12 (1×1) , and Low IRTA = 6 (2×2) . So, out of the total 23 test data, the accurately predicted data was $(0+12+6)/23$, resulting in a GNB accuracy of $(18/23)$ 78.26 percent.

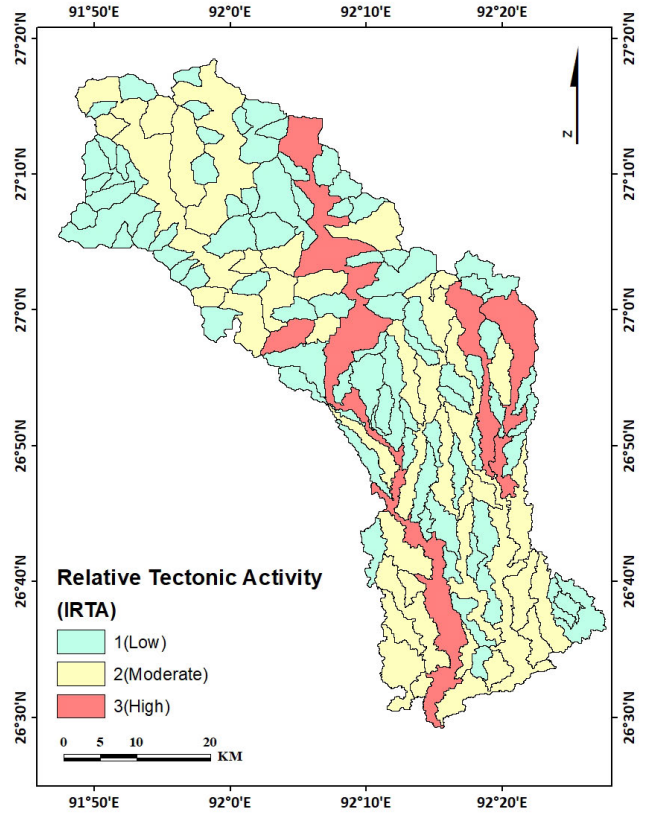


FIGURE 12. Spatial distribution of relative tectonic activity index.

For the selected database SVM algorithm shows the highest accuracy of 82.60% percent for the prediction of the class of IRTA. Additionally, it should be noted that the DT, NB, and ETC showed the similar highest accuracy as SVM; however, the measured F1 score value is not ideal except for SVM. Despite the fact that this work produced greater precision and an excellent F1 score, the proposed SVM-based model has certain drawbacks. One of the major constraints was observed that the dataset contains imbalanced data, such as the difference between the minority class (High IRTA) and majority class (Low IRTA) is very high, which somehow limits the accuracy level of the model.

The primary objective of this research is to examine, assess, and measure the significance of active tectonic processes within the lesser Himalayan zone. Previous evaluations of past tectonic activity have relied on a constrained set of morphometric characteristics [12], [51], [52]. The current study aims to unravel ongoing tectonic activities across a 2404 km^2 area encompassing 115 sub-basins, utilizing linear, areal, and relief-based parameters. The drainage basin delineation utilized the [6] method for stream ordering. The study area's 115 sub-basins exhibit a range of stream orders, from first-order to fifth-order river basins. The count of streams tends to be higher in first-order basins, gradually decreasing as stream order increases. Sub-basins with higher R_b values traverse geological fault lines such as MCT (Main

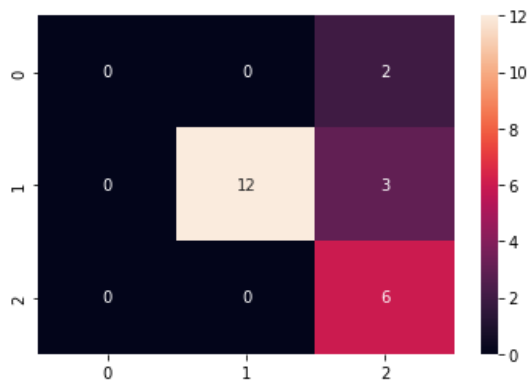


FIGURE 13. Confusion matrix of GNB classifier for predictions the class of IRTA.

Central Thrust), ST (Shurma Thrust), MBT (Main Boundary Thrust), MFT (Main Frontal Thrust), AF (Atherkhet Fault), and KF (Kopili Fault). All computed parameters are classified to discern regions displaying active tectonics. The bifurcation and stream length ratios, two key parameters, are divided into distinct classes. Most of the basins fall within the moderate to highly active tectonics zone. Areal parameters have been assessed, identifying basins within a high activity zone. The evaluation of relief parameters considers relief ratio and ruggedness number. Relief parameters indicating tectonic activity align with the Kopili Fault. Most of the area falls within a low to high active zone regarding relief parameters' tectonic significance.

The key findings of the current study include the following: Subsurface geological features and active subsurface processes have regulated the river's path (Figure 14). According to morphometric results, the drainage network of the basin region was affected by North-West to South-East trending faults. Geomorphic parameter calculations can provide signs of tectonic effect on the development of the terrain. The morphometric analysis of the Dhansiri(North) river basins of the north branch of the Brahmaputra in Assam has demonstrated that specific indices, such as the bifurcation ratio (R_b), stream length ratio (R_L), form factor (F_f), elongation ratio (R_e), relief ratio (R_h), and ruggedness number (R_n), can provide significant information. The co-evaluation of the indices using an integrated index, referred to as the IRTA (Index of Relative Tectonic Activity), might provide insightful information about the relative tectonic activity. The research region was divided into sub-areas of low, moderate, and high relative tectonic activity based on the categorization of the drainage basins into three classifications. Around 68% of the research region is categorised as having low, 23% as having moderate, and 9% as having high tectonic activity. The tectonic structure of the studied region appears to be reflected in the spatial distribution of the values of this new index. In comparison to other drainage systems, the basins of the kopili-dhansiri fault drainage systems exhibit high values of the calculated morphometric indices. This method proved

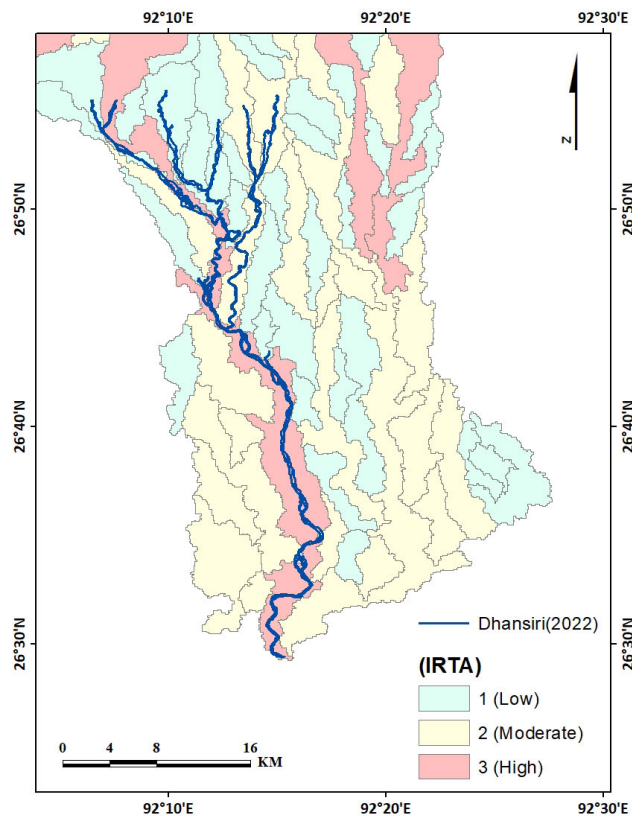


FIGURE 14. Dhansiri(North) river active channel along with the high IRTA zone.

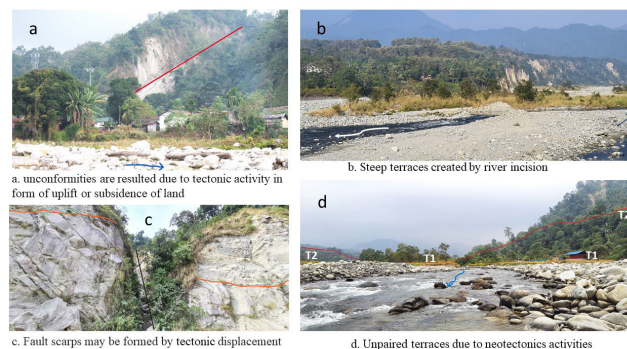


FIGURE 15. Field evidences of Neo-tectonic activities in the part of Dhansiri(North) river basin.

that the estimated values clearly demonstrated the tectonic effect on the drainage systems of the Dhansiri(North) river basin and that the morphometry of the drainage basins formed on the rising block of the major faults is indicative of tectonic activity. The morphometric study done as part of this research did not support the assertion by earlier studies that there was an active fault along the Dhansiri-Kopili Straits. It must be highlighted that the methodology and classification of the relative tectonic activity only reveal relative differences and at a local level since the study as a whole, i.e., the selection of the parameters and the categorization of the drainage basins,



FIGURE 16. Field photos of areas with high relative tectonic activity index.

reflects the local conditions. The accuracy of the IRTA map is evaluated using an existing tectonic map and ML algorithms. Additionally, Field investigations have confirmed the IRTA findings’ interpretation that neotectonic activity caused slope failure, the activation of landslides, earthquakes, and other natural hazards (Figures 15 and 16).

V. CONCLUSION

The role of neotectonics in the part of the Dhansiri(North) river basin is evident from the evaluated morphometric parameters (Linear, Areal, and Relief parameters). These parameters act as a significant tool for determining Index for Relative Tectonic Activity (IRTA). This approach helps in identification of tectonically active zones,where more detailed field studies will identify active structures and calculate rates of active tectonic processes. Based on the IRTA class, the region was divided into three sub-areas with varying levels of tectonic activity. The low, moderate, and high tectonic activity areas were determined by categorizing the drainage basins into three classes. 68% area of the region classified as low, 23% as moderate, and 9% as high tectonic activity. The results of the parameters have a profound role in the neo-tectonics, as major faults like Atherket fault and Dhansiri-kopili fault pass through the basins. The modeling results showed that the SVM algorithm achieved the highest accuracy of 82.60%.It indicates a relatively high level of predictive performance, and also suggesting that the SVM model can effectively distinguish between different classes or categories.The significance of the 82.60% accuracy with the SVM algorithm lies in its ability to provide valuable insights into the predictive capabilities of the model within the specific constraints and requirements of the study.This accuracy rate surpasses the baseline and may be considered satisfactory based on the complexity of the problem under investigation.The implications of this accuracy level extend in two distinct directions. Firstly, it underscores the SVM algorithm’s proficiency within the study’s context, showcasing its capability to make precise predictions. It suggests a high degree of competence in handling the intricacies of the dataset. Secondly, it’s equally important to contextualize this achievement within the broader landscape of the problem domain. Although the achieved accuracy is commendable, it’s important to

TABLE 4. Rank assigned based on morphometric parameters.

RANK OF	RELATIVE TECTONIC ACTIVITY INDEX	LINEAR MORPHOMETRIC PARAMETERS	AREAL MORPHOMETRIC PARAMETERS	RELIEF MORPHOMETRIC PARAMETERS	IRTA CLASS	ACCURACY	IRTA CLASS	ACCURACY
1	1.000	1.000	1.000	1.000	1	0.826	1	0.826
2	1.000	1.000	1.000	1.000	1	0.826	1	0.826
3	1.000	1.000	1.000	1.000	1	0.826	1	0.826
4	1.000	1.000	1.000	1.000	1	0.826	1	0.826
5	1.000	1.000	1.000	1.000	1	0.826	1	0.826
6	1.000	1.000	1.000	1.000	1	0.826	1	0.826
7	1.000	1.000	1.000	1.000	1	0.826	1	0.826
8	1.000	1.000	1.000	1.000	1	0.826	1	0.826
9	1.000	1.000	1.000	1.000	1	0.826	1	0.826
10	1.000	1.000	1.000	1.000	1	0.826	1	0.826
11	1.000	1.000	1.000	1.000	1	0.826	1	0.826
12	1.000	1.000	1.000	1.000	1	0.826	1	0.826
13	1.000	1.000	1.000	1.000	1	0.826	1	0.826
14	1.000	1.000	1.000	1.000	1	0.826	1	0.826
15	1.000	1.000	1.000	1.000	1	0.826	1	0.826
16	1.000	1.000	1.000	1.000	1	0.826	1	0.826
17	1.000	1.000	1.000	1.000	1	0.826	1	0.826
18	1.000	1.000	1.000	1.000	1	0.826	1	0.826
19	1.000	1.000	1.000	1.000	1	0.826	1	0.826
20	1.000	1.000	1.000	1.000	1	0.826	1	0.826
21	1.000	1.000	1.000	1.000	1	0.826	1	0.826
22	1.000	1.000	1.000	1.000	1	0.826	1	0.826
23	1.000	1.000	1.000	1.000	1	0.826	1	0.826
24	1.000	1.000	1.000	1.000	1	0.826	1	0.826
25	1.000	1.000	1.000	1.000	1	0.826	1	0.826
26	1.000	1.000	1.000	1.000	1	0.826	1	0.826
27	1.000	1.000	1.000	1.000	1	0.826	1	0.826
28	1.000	1.000	1.000	1.000	1	0.826	1	0.826
29	1.000	1.000	1.000	1.000	1	0.826	1	0.826
30	1.000	1.000	1.000	1.000	1	0.826	1	0.826
31	1.000	1.000	1.000	1.000	1	0.826	1	0.826
32	1.000	1.000	1.000	1.000	1	0.826	1	0.826
33	1.000	1.000	1.000	1.000	1	0.826	1	0.826
34	1.000	1.000	1.000	1.000	1	0.826	1	0.826
35	1.000	1.000	1.000	1.000	1	0.826	1	0.826
36	1.000	1.000	1.000	1.000	1	0.826	1	0.826
37	1.000	1.000	1.000	1.000	1	0.826	1	0.826
38	1.000	1.000	1.000	1.000	1	0.826	1	0.826
39	1.000	1.000	1.000	1.000	1	0.826	1	0.826
40	1.000	1.000	1.000	1.000	1	0.826	1	0.826
41	1.000	1.000	1.000	1.000	1	0.826	1	0.826
42	1.000	1.000	1.000	1.000	1	0.826	1	0.826
43	1.000	1.000	1.000	1.000	1	0.826	1	0.826
44	1.000	1.000	1.000	1.000	1	0.826	1	0.826
45	1.000	1.000	1.000	1.000	1	0.826	1	0.826
46	1.000	1.000	1.000	1.000	1	0.826	1	0.826
47	1.000	1.000	1.000	1.000	1	0.826	1	0.826
48	1.000	1.000	1.000	1.000	1	0.826	1	0.826
49	1.000	1.000	1.000	1.000	1	0.826	1	0.826
50	1.000	1.000	1.000	1.000	1	0.826	1	0.826
51	1.000	1.000	1.000	1.000	1	0.826	1	0.826
52	1.000	1.000	1.000	1.000	1	0.826	1	0.826
53	1.000	1.000	1.000	1.000	1	0.826	1	0.826
54	1.000	1.000	1.000	1.000	1	0.826	1	0.826
55	1.000	1.000	1.000	1.000	1	0.826	1	0.826
56	1.000	1.000	1.000	1.000	1	0.826	1	0.826
57	1.000	1.000	1.000	1.000	1	0.826	1	0.826
58	1.000	1.000	1.000	1.000	1	0.826	1	0.826
59	1.000	1.000	1.000	1.000	1	0.826	1	0.826
60	1.000	1.000	1.000	1.000	1	0.826	1	0.826
61	1.000	1.000	1.000	1.000	1	0.826	1	0.826
62	1.000	1.000	1.000	1.000	1	0.826	1	0.826
63	1.000	1.000	1.000	1.000	1	0.826	1	0.826
64	1.000	1.000	1.000	1.000	1	0.826	1	0.826
65	1.000	1.000	1.000	1.000	1	0.826	1	0.826
66	1.000	1.000	1.000	1.000	1	0.826	1	0.826
67	1.000	1.000	1.000	1.000	1	0.826	1	0.826
68	1.000	1.000	1.000	1.000	1	0.826	1	0.826
69	1.000	1.000	1.000	1.000	1	0.826	1	0.826
70	1.000	1.000	1.000	1.000	1	0.826	1	0.826
71	1.000	1.000	1.000	1.000	1	0.826	1	0.826
72	1.000	1.000	1.000	1.000	1	0.826	1	0.826
73	1.000	1.000	1.000	1.000	1	0.826	1	0.826
74	1.000	1.000	1.000	1.000	1	0.826	1	0.826
75	1.000	1.000	1.000	1.000	1	0.826	1	0.826
76	1.000	1.000	1.000	1.000	1	0.826	1	0.826
77	1.000	1.000	1.000	1.000	1	0.826	1	0.826
78	1.000	1.000	1.000	1.000	1	0.826	1	0.826
79	1.000	1.000	1.000	1.000	1	0.826	1	0.826
80	1.000	1.000	1.000	1.000	1	0.826	1	0.826
81	1.000	1.000	1.000	1.000	1	0.826	1	0.826
82	1.000	1.000	1.000	1.000	1	0.826	1	0.826
83	1.000	1.000	1.000	1.000	1	0.826	1	0.826
84	1.000	1.000	1.000	1.000	1	0.826	1	0.826
85	1.000	1.000	1.000	1.000	1	0.826	1	0.826
86	1.000	1.000	1.000	1.000	1	0.826	1	0.826
87	1.000	1.000	1.000	1.000	1	0.826	1	0.826
88	1.000	1.000	1.000	1.000	1	0.826	1	0.826
89	1.000	1.000	1.000	1.000	1	0.826	1	0.826
90	1.000	1.000	1.000	1.000	1	0.826	1	0.826
91	1.000	1.000	1.000	1.000	1	0.826	1	0.826
92	1.000	1.000	1.000	1.000	1	0.826	1	0.826
93	1.000	1.000	1.000	1.000	1	0.826	1	0.826
94	1.000	1.000	1.000	1.000	1	0.826	1	0.826
95	1.000	1.000	1.000	1.000	1	0.826	1	0.826
96	1.000	1.000	1.000	1.000	1	0.826	1	0.826
97	1.000	1.000	1.000	1.000	1	0.826	1	0.826
98	1.000	1.000	1.000	1.000	1	0.826	1	0.826
99	1.000	1.000	1.000	1.000	1	0.826	1	0.826
100	1.000	1.000	1.000	1.000	1	0.826	1	0.826

recognize that it’s not a definitive measure of success. Rather, it provides valuable insights into the predictive abilities of the SVM model under the specific constraints and requirements outlined in the study.Evaluating accuracy within the broader problem context facilitates a deeper understanding of the model’s performance and potential implications for real-world applications. Therefore, the significance of achieving an 82.60 percent accuracy with the SVM algorithm lies not only in its immediate predictive prowess but also in its capacity to provide nuanced insights into the broader predictive landscape of the problem domain. A comparison of field observations for understanding the imprints of active tectonics on the basin area coincides with the values and classes of morphometric indices and the overall IRTA index. This area with moderate to high relative tectonic activity index corresponds with areas where prominent fault scarps, triangular facets, unpaired terraces, and deformed alluvial fan deposits are shown. Additional in-depth analysis of the Quaternary chronology and significant displacements will be effective in the future.Our results cover the vital gap in neotectonics, showing evidence in unstudied sectors of the northern part of the Brahmaputra basin area in the lower Assam region. Morphometric analysis, combined with the Index of Relative Tectonic Activity (IRTA) and machine learning techniques, plays a crucial role in identifying the underlying causes of major disasters such as earthquakes, floods, and landslides and identifying hazard-prone areas. This knowledge can then suggest suitable remedial measures for disaster mitigation, such as land use planning,

TABLE 5. Classification of IRTA(Index of Relative Tectonic Activity) in the Sub basins of Dhansiri(North) river basin.

BASIN_ID	Class (Rb)	Class (RL)	Class (Ff)	Class (Re)	Class (Rh)	Class (Rn)	If _s =S/n	class (IRTA)
1	1	2	2	2	1	1	1.5	2
2	1	1	2	2	1	1	1.33333333	2
3	1	1	1	1	1	1	1	1
4	1	1	1	1	1	1	1	1
5	1	1	2	1	1	1	1.16666667	1
6	2	2	2	1	1	1	1.5	2
7	1	1	1	1	1	1	1	1
8	1	1	1	1	1	1	1	1
9	1	1	1	1	1	2	1.16666667	1
10	1	1	1	1	2	2	1.33333333	2
11	2	2	1	1	2	2	1.66666667	3
12	1	1	2	1	1	1	1.16666667	1
13	1	1	1	1	1	1	1	1
14	1	1	1	1	1	1	1	1
15	1	1	1	1	1	1	1	1
16	2	2	1	1	1	1	1.33333333	2
17	1	1	1	1	1	1	1	1
18	1	1	1	1	1	1	1	1
19	1	1	2	1	1	1	1.16666667	1
20	1	1	2	1	1	1	1.16666667	1
21	2	2	1	1	1	1	1.33333333	2
22	2	1	1	1	1	1	1.16666667	1
23	1	1	1	1	1	1	1	1
24	1	1	1	1	1	1	1	1
25	1	1	1	1	1	1	1	1
26	1	1	1	1	1	1	1	1
27	1	1	1	1	1	1	1	1
28	1	1	1	1	1	1	1	1
29	1	2	1	1	1	1	1.16666667	1
30	2	1	1	1	1	1	1.16666667	1
31	2	1	2	2	2	2	1.83333333	3
32	2	2	2	2	2	2	1.83333333	3
33	1	1	2	2	1	1	1.33333333	2
34	1	1	2	2	1	1	1.33333333	2
35	1	1	2	2	1	1	1.33333333	2
36	1	1	2	2	1	1	1.33333333	2
37	1	1	2	2	1	1	1.33333333	2
38	2	1	2	2	1	1	1.5	2
39	2	1	2	1	1	1	1.33333333	2
40	1	1	2	2	1	1	1.33333333	2
41	2	2	1	1	1	1	1.33333333	2
42	1	1	1	1	2	1	1.16666667	1
43	1	1	1	1	1	1	1	1
44	2	2	1	1	2	1	1.5	2
45	1	2	1	1	1	1	1.16666667	1
46	1	1	1	1	1	1	1	1
47	1	1	1	1	1	1	1	1
48	1	1	1	1	1	1	1	1
49	1	1	1	1	1	1	1	1
50	1	2	1	1	1	2	1.33333333	2
51	1	1	1	1	1	1	1	1
52	1	1	1	1	1	1	1	1
53	1	1	1	1	1	1	1	1
54	1	1	1	1	1	1	1	1
55	2	1	1	1	1	1	1.16666667	1
56	2	2	1	1	1	2	1.5	2
57	1	1	1	1	1	1	1	1
58	2	1	1	1	1	1	1.16666667	1
59	1	2	1	1	2	1	1.33333333	2
60	1	1	1	1	2	1	1.16666667	1
61	2	1	1	1	1	1	1.16666667	1
62	1	1	1	1	1	1	1	1
63	1	1	1	1	1	1	1	1
64	1	1	1	1	1	1	1	1
65	1	1	1	1	1	1	1	1
66	1	1	1	1	1	1	1	1
67	1	1	1	1	1	1	1	1
68	1	2	1	1	1	1	1.16666667	1
69	1	1	1	1	1	1	1	1
70	2	2	1	1	1	1	1.33333333	2
71	1	1	1	1	1	1	1	1
72	1	1	1	1	2	2	1.33333333	2
73	1	1	1	1	1	1	1	1
74	1	1	1	1	1	1	1	1
75	1	1	2	2	1	1	1.33333333	2
76	1	1	2	2	1	1	1.33333333	2
77	1	1	2	2	1	1	1.33333333	2
78	2	1	2	1	1	1	1.33333333	2
79	2	2	2	1	2	2	1.83333333	3
80	2	1	1	1	1	1	1.16666667	1
81	1	1	1	1	1	1	1	1
82	1	1	1	1	1	1	1	1
83	1	2	1	1	1	1	1.16666667	1
84	1	1	1	1	1	1	1	1
85	1	2	1	1	1	1	1.16666667	1
86	1	2	1	1	1	1	1.16666667	1
87	1	1	1	1	1	1	1	1
88	1	1	1	1	1	1	1	1
89	1	2	1	1	1	1	1.16666667	1
90	2	2	1	1	1	2	1.5	2
91	1	1	1	1	1	1	1.16666667	1
92	1	1	1	1	1	1	1	1
93	2	1	1	1	1	1	1.16666667	1
94	1	1	1	1	1	1	1	1
95	1	1	1	1	1	1	1	1
96	2	1	1	1	1	1	1.16666667	1
97	2	1	1	1	1	1	1.16666667	1
98	1	1	1	1	1	1	1	1
99	2	2	1	1	1	2	1.5	2
100	2	1	1	1	1	2	1.33333333	2
101	1	1	1	1	1	2	1.16666667	1
102	1	1	1	1	1	2	1.16666667	1
103	1	2	1	1	1	1	1.16666667	1
104	1	1	1	1	1	2	1.16666667	1
105	2	2	1	1	1	2	1.5	2
106	1	1	1	1	1	1	1	1
107	1	1	1	1	1	2	1.16666667	1
108	1	1	1	1	1	1	1	1
109	1	2	1	1	1	1	1.16666667	1
110	2	1	1	1	1	2	1.33333333	2
111	2	1	1	1	1	1	1.16666667	1
112	2	2	1	1	1	1	1.33333333	2
113	2	1	1	1	1	1	1.16666667	1
114	1	1	1	1	2	2	1.33333333	2
115	2	1	1	1	2	2	1.5	2

infrastructure development, and early warning systems, ultimately reducing disaster risk and protecting vulnerable communities. This study holds promise for enhancing our

ability to mitigate the impacts of natural disasters and protect vulnerable communities and infrastructure.

ACKNOWLEDGMENT

The authors extend their appreciation to the Researchers Supporting Project, King Saud University, Saudi Arabia for funding this research work through the project No. RSPD2024R951.

APPENDIX

See Tables 4 and 5.

REFERENCES

- [1] S. Ouchi, "Response of alluvial rivers to slow active tectonic movement," *Geolog. Soc. Amer. Bull.*, vol. 96, no. 4, pp. 504–515, 1985.
- [2] A. Goudie, *Encyclopedia of Geomorphology*, vol. 2. London, U.K.: Routledge, 2004.
- [3] I. S. Evans, "Geomorphometry and landform mapping: What is a landform?" *Geomorphology*, vol. 137, no. 1, pp. 94–106, Jan. 2012.
- [4] R. E. Horton, "Drainage-basin characteristics," *Trans., Amer. Geophys. Union*, vol. 13, no. 1, pp. 350–361, 1932.
- [5] R. E. Horton, "Erosional development of streams and their drainage basins; hydrophysical approach to quantitative morphology," *Geolog. Soc. Amer. Bull.*, vol. 56, no. 3, pp. 275–370, 1945.
- [6] A. N. Strahler, "Quantitative analysis of watershed geomorphology," *Eos, Trans. Amer. Geophys. Union*, vol. 38, no. 6, pp. 913–920, 1957.
- [7] J. I. Clarke, *Morphometry From Maps, Essays in Geomorphology*, vol. 252. Amsterdam, The Netherlands: Elsevier, 1966, pp. 235–274.
- [8] J. Clarke, *Morphometry From Maps. Essays in Geomorphology*. New York, NY, USA: Elsevier, 1996.
- [9] C. G. Chase, "Tectonic history of the Fiji Plateau," *Geolog. Soc. Amer. Bull.*, vol. 82, no. 11, pp. 3087–3110, 1971.
- [10] J. T. Hack, "Stream-profile analysis and stream-gradient index," *J. Res. United States Geolog. Surv.*, vol. 1, no. 4, pp. 421–429, 1973.
- [11] E. A. Keller and N. Pinter, *Active Tectonics*, vol. 338. Upper Saddle River, NJ, USA: Prentice-Hall, 1996.
- [12] R. El Hamdouni, C. Irigaray, T. Fernández, J. Chacón, and E. A. Keller, "Assessment of relative active tectonics, southwest border of the Sierra Nevada (Southern Spain)," *Geomorphology*, vol. 96, nos. 1–2, pp. 150–173, Apr. 2008.
- [13] A. Habibi and M. Gharibreza, "Estimation of the relative active tectonics in Shahriary basin (Central Iran) using geomorphic and seismicity indices," *Natural Environ. Change*, vol. 1, no. 1, pp. 71–83, 2015.
- [14] P. D. Jacques, E. D. Salvador, R. Machado, C. H. Grohmann, and A. R. Nummer, "Application of morphometry in neotectonic studies at the eastern edge of the Paraná basin, Santa Catarina State, Brazil," *Geomorphology*, vol. 213, pp. 13–23, May 2014.
- [15] W. B. Bull and L. D. McFadden, "Tectonic geomorphology north and south of the Garlock fault, California," in *Geomorphology in Arid Regions*. Evanston, IL, USA: Routledge, 2020, pp. 115–138.
- [16] T. Rockwell, E. Keller, and D. Johnson, "Tectonic geomorphology of alluvial fans and mountain fronts near Ventura, California, tectonic geomorphology," in *Proc. 15th Annu. Geomorphol. Symp.* Boston, MA, USA: Allen and Unwin, 1985, pp. 183–207.
- [17] P. G. Silva, J. Goy, C. Zazo, and T. Bardaji, "Fault-generated mountain fronts in Southeast Spain: Geomorphologic assessment of tectonic and seismic activity," *Geomorphology*, vol. 50, nos. 1–3, pp. 203–225, 2003.
- [18] F. Ferraris, M. Firpo, and F. J. Pazzaglia, "DEM analyses and morphotectonic interpretation: The Plio-Quaternary evolution of the Eastern Ligurian Alps, Italy," *Geomorphology*, vols. 149–150, pp. 27–40, May 2012.
- [19] S. A. Mahmood and R. Gloaguen, "Appraisal of active tectonics in Hindu Kush: Insights from DEM derived geomorphic indices and drainage analysis," *Geosci. Frontiers*, vol. 3, no. 4, pp. 407–428, Jul. 2012.
- [20] N. Bagha, M. Arian, M. Ghorashi, M. Pourkermani, R. El Hamdouni, and A. Solgi, "Evaluation of relative tectonic activity in the Tehran basin, Central Alborz, Northern Iran," *Geomorphology*, vol. 213, pp. 66–87, May 2014.
- [21] H. H. Hosseinlou, "Morphotectonics investigations of the Garehbagh basin area based on morphometric indices, NW Iran," *Iranian J. Earth Sci.*, vol. 9, no. 2, pp. 105–114, Jan. 2017.

- [22] K. Buczek and M. Górnik, "Evaluation of tectonic activity using morphometric indices: Case study of the Tatra Mts. (Western Carpathians, Poland)," *Environ. Earth Sci.*, vol. 79, no. 8, p. 176, Apr. 2020.
- [23] L. Burian, A. V. Mitusov, and J. Poesen, "Relationships of attributes of gullies with morphometric variables," *Geomorphometry*, vol. 1, pp. 111–114, Jan. 2015.
- [24] M. Softa, T. Emre, H. Sözbilir, J. Q. G. Spencer, and M. Turan, "Geomorphic evidence for active tectonic deformation in the coastal part of Eastern Black Sea, Eastern Pontides, Turkey," *Geodinamica Acta*, vol. 30, no. 1, pp. 249–264, Jan. 2018.
- [25] K. Valkanou, E. Karymbalis, D. Papanastassiou, M. Soldati, C. Chalkias, and K. Gaki-Papanastassiou, "Morphometric analysis for the assessment of relative tectonic activity in Evia Island, Greece," *Geosciences*, vol. 10, no. 7, p. 264, Jul. 2020.
- [26] A. Lone, "Morphometric and morphotectonic analysis of Ferozpur drainage basin left bank Tributary of River Jhelum of Kashmir Valley, NW Himalayas, India," *J. Geography Natural Disasters*, vol. 7, no. 3, 2017, Art. no. 1000208.
- [27] A. K. Anand and S. P. Pradhan, "Assessment of active tectonics from geomorphic indices and morphometric parameters in part of Ganga basin," *J. Mountain Sci.*, vol. 16, no. 8, pp. 1943–1961, Aug. 2019.
- [28] R. S. Kandregula, G. C. Kothiyari, K. Swamy, and S. Rawat, "Quantitative assessment of tectonic activity in Northern Saurashtra, Western India," *J. Indian Geophys. Union*, vol. 23, no. 6, pp. 542–558, 2019.
- [29] C. S. Agarwal, "Study of drainage pattern through aerial data in Naugarh area of Varanasi district, UP," *J. Indian Soc. Remote Sens.*, vol. 26, no. 4, pp. 169–175, Dec. 1998.
- [30] K.-T. Chang, A. Merghadi, A. P. Yunus, B. T. Pham, and J. Dou, "Evaluating scale effects of topographic variables in landslide susceptibility models using GIS-based machine learning techniques," *Sci. Rep.*, vol. 9, no. 1, p. 12296, 2019.
- [31] F. Guzzetti, A. Carrara, M. Cardinali, and P. Reichenbach, "Landslide hazard evaluation: A review of current techniques and their application in a multi-scale study, Central Italy," *Geomorphology*, vol. 31, nos. 1–4, pp. 181–216, Dec. 1999.
- [32] S. Lee and B. Pradhan, "Landslide hazard mapping at Selangor, Malaysia using frequency ratio and logistic regression models," *Landslides*, vol. 4, no. 1, pp. 33–41, Feb. 2007.
- [33] A. Akgun and N. Türk, "Landslide susceptibility mapping for Ayvalik (Western Turkey) and its vicinity by multicriteria decision analysis," *Environ. Earth Sci.*, vol. 61, no. 3, pp. 595–611, Aug. 2010.
- [34] C. Gokceoglu, H. Sonmez, and M. Ercanoglu, "Discontinuity controlled probabilistic slope failure risk maps of the Altindag (settlement) region in Turkey," *Eng. Geol.*, vol. 55, no. 4, pp. 277–296, Mar. 2000.
- [35] S. Lee and B. Pradhan, "Probabilistic landslide hazards and risk mapping on Penang Island, Malaysia," *J. Earth Syst. Sci.*, vol. 115, no. 6, pp. 661–672, Dec. 2006.
- [36] H. R. Pourghasemi, H. R. Moradi, and S. M. F. Aghda, "Landslide susceptibility mapping by binary logistic regression, analytical hierarchy process, and statistical index models and assessment of their performances," *Natural Hazards*, vol. 69, no. 1, pp. 749–779, Oct. 2013.
- [37] T. V. Swetha, G. Gopinath, A. Bhadrans, and P. Arjun, "Geospatial approach to elucidate anomalies in the hierarchical organization of drainage network in Kuttiyadi River Basin, Southern India," *Frontiers Earth Sci.*, vol. 16, no. 3, pp. 786–797, Sep. 2022.
- [38] G. Girish, A. G. Kamalamma, N. P. Jesiya, and K. Lemoon, "Hydro-hypsometric analysis of tropical river basins, southwest coast of India using geospatial technology," *J. Mountain Sci.*, vol. 13, no. 5, pp. 939–946, May 2016.
- [39] C. M. P. Souza, N. A. Figueredo, L. M. Costa, G. V. Veloso, M. I. S. Almeida, and E. J. Ferreira, "Machine learning algorithm in the prediction of geomorphic indices for appraisal the influence of landscape structure on fluvial systems, Southeastern–Brazil," *Revista Brasileira de Geomorfologia*, vol. 21, no. 2, pp. 365–380, Apr. 2020.
- [40] A. Khakpour and R. Colomo-Palacios, "Convergence of gamification and machine learning: A systematic literature review," *Technol., Knowl. Learn.*, vol. 26, no. 3, pp. 597–636, Sep. 2021.
- [41] G. M. Foody and A. Mathur, "Toward intelligent training of supervised image classifications: Directing training data acquisition for SVM classification," *Remote Sens. Environ.*, vol. 93, nos. 1–2, pp. 107–117, Oct. 2004.
- [42] J. Ham, Y. Chen, M. M. Crawford, and J. Ghosh, "Investigation of the random forest framework for classification of hyperspectral data," *IEEE Trans. Geosci. Remote Sens.*, vol. 43, no. 3, pp. 492–501, Mar. 2005.
- [43] M. Pal and P. M. Mather, "Support vector machines for classification in remote sensing," *Int. J. Remote Sens.*, vol. 26, no. 5, pp. 1007–1011, Mar. 2005.
- [44] J. A. Lee, M. C. Baddock, M. J. Mbu, and T. E. Gill, "Geomorphic and land cover characteristics of aeolian dust sources in West Texas and Eastern New Mexico, USA," *Aeolian Res.*, vol. 3, no. 4, pp. 459–466, Jan. 2012.
- [45] V. Liesenberg and R. Gloaguen, "The impact of precipitation events on forest classification using multitemporal ALOS/PALSAR data," *ESA Special Publication*, vol. 56, p. 713, Aug. 2013.
- [46] B. Waske, J. A. Benediktsson, and J. R. Sveinsson, "Classifying remote sensing data with support vector machines and imbalanced training data," in *Proc. 8th Int. Workshop Multiple Classifier Syst.*, vol. 8, Reykjavik, Iceland, Jun. 2009, pp. 375–384.
- [47] L. Yu, A. Porwal, E.-J. Holden, and M. C. Dentith, "Towards automatic lithological classification from remote sensing data using support vector machines," *Comput. Geosci.*, vol. 45, pp. 229–239, Aug. 2012.
- [48] A. Othman and R. Gloaguen, "Improving lithological mapping by SVM classification of spectral and morphological features: The discovery of a new chromite body in the Mawat ophiolite complex (Kurdistan, NE Iraq)," *Remote Sens.*, vol. 6, no. 8, pp. 6867–6896, Jul. 2014.
- [49] M. J. Cracknell and A. M. Reading, "Geological mapping using remote sensing data: A comparison of five machine learning algorithms, their response to variations in the spatial distribution of training data and the use of explicit spatial information," *Comput. Geosci.*, vol. 63, pp. 22–33, Feb. 2014.
- [50] S. A. Schumm, "Evolution of drainage systems and slopes in Badlands at Perth Amboy, New Jersey," *Geol. Soc. Amer. Bull.*, vol. 67, no. 5, pp. 597–646, 1956.
- [51] W. Bull and L. McFadden, "Tectonic geomorphology of north and south of the Garlock fault, California," *J. Geomorphol.*, vol. 1, pp. 15–32, Sep. 1977.
- [52] A. Azor, E. A. Keller, and R. S. Yeats, "Geomorphic indicators of active fold growth: South Mountain–Oak Ridge Anticline, Ventura Basin, Southern California," *Geol. Soc. Amer. Bull.*, vol. 114, no. 6, pp. 745–753, Jun. 2002.



SHAYANI ROY received the B.Sc. and M.Sc. degrees in geography from the University of Calcutta, in 2015 and 2017, respectively. She is currently a Senior Research Fellow with the Department of Earth Sciences, Indian Institute of Engineering Science and Technology, Shibpur. Her research interests include geomorphology, river dynamics, tectonic settings, fluvial sediments, and quaternary environment.



PRITAM MANDAL received the M.Tech. degree from the Dr. M. N. Dastur School of Materials Science and Engineering, Indian Institute of Engineering Science and Technology (IIEST), Shibpur, India, in 2020. He is currently pursuing the Ph.D. degree with the Department of Metallurgy and Materials Engineering, IIEST, Shibpur. His research interests include machine learning and surface engineering.



AMITAVA CHOWDHURY received the M.Tech. degree from Jadavpur University, India, in 2013, and the Ph.D. degree from Indian Institute of Engineering science and Technology, Shibpur (formerly BESU, Shibpur), in 2020. He is currently an Assistant Professor with the Department of Computer Science and Engineering, Pandit Deendayal Energy University, Gandhinagar, Gujarat, India. His research interests include computational geometry in the field of micromechanical modeling, pattern recognition, character recognition, and machine learning.



AYAN H. SEIKH is currently pursuing the B.Tech. degree in computer science and engineering with the Motilal Nehru National Institute of Technology Allahabad, Prayagraj, India.



cloud computing, recommender systems, data analytics, software engineering, and sensor.

M. ABDULLAH-AL-WADUD received the B.S. and M.S. degrees in computer science and engineering from the University of Dhaka, Bangladesh, in 2003 and 2004, respectively, and the Ph.D. degree in computer engineering from Kyung Hee University, South Korea, in 2009. He is currently an Associate Professor with the Department of Software Engineering, King Saud University, Saudi Arabia. His research interests include pattern recognition, optimization, computer vision,



MANOJIT GHOSH received the M.Tech. degree from IIT Kharagpur and the Ph.D. degree from Delft University of Technology, The Netherlands. He is currently a Professor with the Department of Metallurgy and Materials Engineering, Indian Institute of Engineering science and Technology (IEST), Shibpur. His research interests include structure-property correlation, thermo-mechanical simulations of non-ferrous metals and alloys, and composite materials.



ARIYAN H. SEIKH is currently pursuing the B.Tech. degree in computer science and engineering with the Motilal Nehru National Institute of Technology Allahabad, Prayagraj, India.



ANANYA MUKHOPADHYAY received the M.Sc. and Ph.D. degrees in geology from the University of Calcutta, in 2019 and 2020, respectively. She is currently a Professor with the Department of Earth Sciences, Indian Institute of Engineering science and Technology (IEST), Shibpur. Her research interests include sedimentary dynamics, basin evolution, and tectonic settings.

...